SAND2016-12286C

Simulations of Realistic Multifunctional Nanoantenna Enabled Detectors

Salvatore Campione, Larry K. Warne, Roy E. Jorgenson
Electromagnetic Theory Department
Sandia National Laboratories
Albuquerque, NM, USA
sncampi@sandia.gov, lkwarne@sandia.gov, rejorge@sandia.gov

Paul S. Davids, David W. Peters
Applied Photonic Microsystems Department
Sandia National Laboratories
Albuquerque, NM, USA
pdavids@sandia.gov, dwpeter@sandia.gov

***Abstract*—The goal of this paper is to investigate full-wave simulations of realistic implementations of multifunctional nanoantenna enabled detectors (NEDs). We realize a 2x2 pixelated array structure that supports two wavelengths of operation. After designing each resonating structure independently using full-wave simulations with periodic boundary conditions mimicking the whole infinite array, we construct a supercell made of a 2x2 pixelated array with periodic boundary conditions mimicking the full NED. In the NED, each pixel comprises 10-20 nanoantennas. Our simulations account for the cross-talk between contiguous pixels. We observe that, even though there are finite extent effects, the pixels work as designed, each responding at the respective wavelength of operation. We want to stress that realistic simulations of multifunctional NEDs need to be performed to verify the design functionality by taking into account finite extent and cross-talk effects.**

Keywords—multifunctional detectors; nanoantenna enabled detectors; finite extent; cross-talk.

I. INTRODUCTION

Tremendous progress has been made in the last decade on infrared detector arrays based on narrow bandgap, III-V semiconductors [1]. Semiconductors containing antimony have enabled certain heterostructures to exhibit a broken gap that is advantageous in some newer detector designs [2, 3]. These narrow bandgap semiconductors show good promise in electronic applications such as high-frequency, low-noise high-electron-mobility-transistors [4]. Highly doped semiconductor materials have also been explored as alternative plasmonic materials [5-7].

Infrared detection has recently been enhanced through the use of plasmonic nanoantenna arrays on top of semiconductor heterostructures that contain the active material of a photodetector [8-10] [see schematic in Fig. 1(a)]. We define these detectors as *nanoantenna enabled detectors* (NEDs). Enhanced fields are generated by the nanoantenna arrays, which in turn induce enhanced absorption within the active material of a photodetector, enhancing its overall performance. Such a nanoantenna array is usually designed by using full-wave simulations of a single resonator employing periodic boundary conditions: this kind of simulation mimics an infinitely extended array.

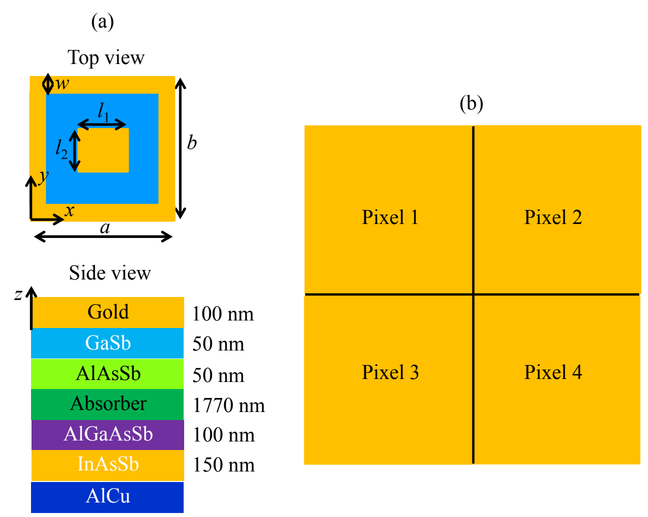

Fig. 1. (a) Illustration of a unit cell of a gold nanoantenna array, together with the semiconductor heterostructure. Periods a and b, patch sides l_1 and l_2, and width w. (b) Illustration of a multifunctional nanoantenna enabled detector made of a 2x2 pixel array, where each pixel is composed of a different, finite nanoantenna array and may perform a different functionality.

In general, there is the need to have multifunctional detectors, and this can be potentially realized using NEDs. Two alternative options exist: (1) one NED that can change its performance via external stimuli, such as a bias voltage; and (2) multiple NEDs interleaved in space [see schematic in Fig. 1(b), also referred to as pixelated arrays], where each pixel is designed to perform different functionalities. While the former is a very attractive platform, the difficulties that are inherent to such a tunable design make the use of pixelated arrays the most viable present solution for multifunctional NEDs. Functionalities may include different polarization properties, different spectral properties, etc. In this paper, we focus on modeling dual-band NEDs made of pixelated arrays. While each resonating structure can be independently designed using full-wave simulations with periodic boundary conditions, there is no guarantee that a pixelated array would perform as desired. This is because the extent of each pixel is finite and thus comprises a finite number of unit cells and may not fulfill the infinite condition imposed by the periodic boundary conditions; and the cross-talk between contiguous pixels may dramatically affect the NED performance. It is our intent to stress that realistic simulations of multifunctional NEDs need to be performed to verify the design functionality and improve their performance.

II. Realistic Dual-Band Nanoantenna Enabled Detectors

We aim to design an NED structure that contains subpixels that work at different wavelengths. For simplicity of discussion, we focus on 4 pixels, displaced in a 2x2 pixelated array in a checker pattern as in Fig. 1(b) and Fig. 2(a), where each diagonal pair works at two different wavelengths: 1) pixel 2 and pixel 3 contain 10 unit cells and work at ~10 μm, with $a = b = 1500$ nm, $l_1 = l_2 = 900$ nm and $w = 50$ nm; and 2) pixel 1 and pixel 4 contain 18 unit cells and work at ~8 μm with $a = b = 800$ nm, $l_1 = l_2 = 150$ nm and $w = 50$ nm.

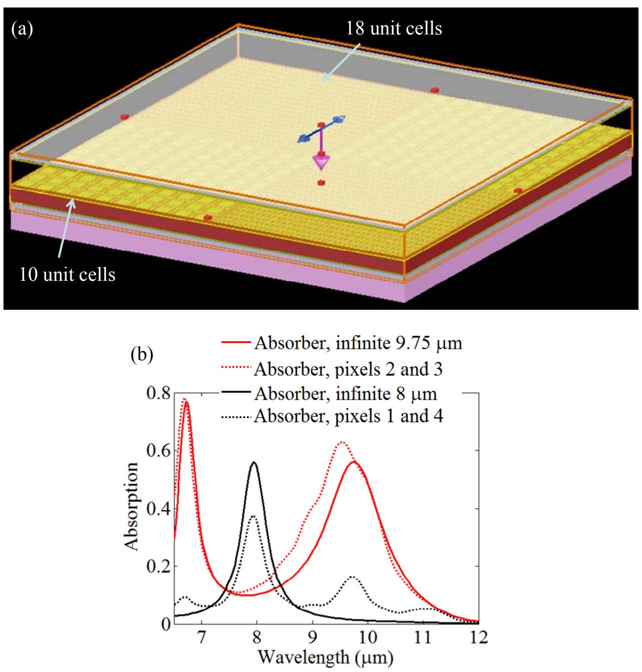

Fig. 2. (a) Illustration of the 2x2 pixelated array NED in checker pattern. Note the finite extent of each pixel. (b) Absorption spectrum of the dual-band detector, highlighting the contributions of main-diagonal and anti-diagonal pixels separately (dotted lines). The results are compared to the infinite arrays (solid lines).

Because of the finite extent of each pixel, it is of interest to determine if the detector will behave as designed, or rather if the optical properties would be dramatically affected by cross-talk between the different pixels. We thus plot in Fig. 2(b) the absorption spectrum of the dual-band detector in Fig. 2(a), restricting the contributions to the main-diagonal (pixels 1 and 4) and anti-diagonal pixels (pixels 2 and 3) separately. One can see that the pixels supporting the resonance at ~10 μm behave better than designed, given that the absorber receives more power (see solid versus dotted red curves). Some minor finite extent and cross-talk effects are observed as a shoulder at ~9 μm. When looking at the result relative to the pixels supporting the resonance at ~8 μm, we see that they behave worse than designed. In particular, we see that the absorber receives less power, and absorbs in frequency bands where it shouldn't, due to evident finite extent and cross-talk effects. Nonetheless, the overall behavior of the NED array is satisfactory, and these realistic simulations can be used to assess (and possibly improve) NED performance.

III. Conclusion

In this paper we have investigated full-wave simulations of realistic implementations of multifunctional nanoantenna enabled detectors. It is pivotal to simulate the entire detector comprising finite extent pixels to correctly account for the cross-talk between contiguous pixels. Even though there are finite extent and cross-talk effects affecting the performance of the dual-band NED under analysis, the pixels work as designed, each responding at the respective wavelength of operation. However, realistic simulations of multifunctional detectors need to be performed to verify the design functionality by taking into account finite extent and cross-talk effects.

Acknowledgment

This work was supported by the Laboratory Directed Research and Development program at Sandia National Laboratories. Sandia National Laboratories is a multi-mission laboratory managed and operated by Sandia Corporation, a wholly owned subsidiary of Lockheed Martin Corporation, for the U.S. Department of Energy's National Nuclear Security Administration under contract DE-AC04-94AL85000.

References

[1] N. K. Dhar, R. Dat, and A. K. Sood, "Advances in Infrared Detector Array Technology," in Optoelectronics - Advanced Materials and Devices, S. L. Pyshkin and J. M. Ballato, Eds., ed: InTech, 2013.

[2] P. Martyniuk, M. Kopytko, and A. Rogalski, "Barrier infrared detectors," Opto Electron. Rev., vol. 22, pp. 127-146, 2014.

[3] E. A. Plis, "InAs/GaSb Type-II Superlattice Detectors," Adv. Electron., vol. 2014, p. 12, 2014.

[4] C. Liu, Y. Li, and Y. Zeng, "Progress in Antimonide Based III-V Compound Semiconductors and Devices," Engineering, vol. 2, pp. 617-624, 2010.

[5] S. Law, R. Liu, and D. Wasserman, "Doped semiconductors with band-edge plasma frequencies," J. Vac. Sci. Technol. B, vol. 32, p. 052601, 2014.

[6] D. Wei, C. Harris, C. C. Bomberger, J. Zhang, J. Zide, and S. Law, "Single-material semiconductor hyperbolic metamaterials," Opt. Express, vol. 24, pp. 8735-8745, 2016.

[7] S. Law, D. C. Adams, A. M. Taylor, and D. Wasserman, "Mid-infrared designer metals," Opt. Express, vol. 20, pp. 12155-12165, 2012.

[8] D. W. Peters, C. M. Reinke, P. S. Davids, J. F. Klem, D. Leonhardt, J. R. Wendt, et al., "Nanoantenna-enabled midwave infrared focal plane arrays," 2012, pp. 83533B-6.

[9] S. Choi and K. Sarabandi, "Bowtie nanoantenna integrated with indium gallium arsenide antimonide for uncooled infrared detector with enhanced sensitivity," Appl. Opt., vol. 52, pp. 8432-8438, 2013.

[10] D. W. Peters, P. S. Davids, J. K. Kim, D. Leonhardt, T. E. Beechem, S. W. Howell, et al., "Application of plasmonic subwavelength structuring to enhance infrared detection," 2014, pp. 899419-6.